

# An integrated optical oxygen sensor fabricated using rapid-prototyping techniques

David A. Chang-Yen and Bruce K. Gale

50 South Central Campus Drive, Room 2240, Department of Mechanical Engineering,  
University of Utah, Salt Lake City, UT 84116, USA. E-mail: dac10@utah.edu;  
Fax: 801-585-9826; Tel: 801-585-3176

Received 13th May 2003, Accepted 28th July 2003

First published as an Advance Article on the web 12th August 2003

This paper details the design and fabrication of an integrated optical biochemical sensor using a select oxygen-sensitive fluorescent dye, tris(2,2'-bipyridyl) dichlororuthenium(II) hexahydrate, combined with polymeric waveguides that are fabricated on a glass substrate. The sensor uses evanescent interaction of light confined within the waveguide with the dye that is immobilized on an SU-8 waveguide surface. Adhesion of the dye to the integrated waveguide surface is accomplished using a unique process of spin-coating/electrostatic layer-by-layer formation. The SU-8 waveguide was chemically modified to allow the deposition process. Exposure of the dye molecules to the analyte and subsequent chemical interaction is achieved by directly coupling the fluid channel to the integrated waveguide. The completed sensor was linear in the dissolved oxygen across a wide range of interest and had a sensitivity of 0.6 ppm. A unique fabrication aspect of this sensor is the inherent simplicity of the design, and the resulting rapidity of fabrication, while maintaining a high degree of functionality and flexibility.

## Introduction and theory

In existing analysis systems, traditional biochemical sensing has been carried out using “extract and evaluate” procedures, where a sample is removed from the system of interest and analyzed to determine the components present, both qualitatively and quantitatively, usually with macroscale equipment in a laboratory situation. This process is time-consuming, limited in application and can be very expensive depending on the difficulty of the extraction process. Sample extraction from an established microsystem would require either alteration of the system design to incorporate a sample exit point, or halting the process and opening the unit to remove the sample material. The latter technique would in most cases require destruction of the microsystem, and both processes will cause severe operational interference and sampling-induced error. Particularly in the case of oxygen sensing or another relatively unstable analyte, the retrieval process itself would most likely irreversibly alter characteristics of the sample, rendering the test useless.

### 1.1 Existing sensing techniques

Applications of microscale dissolved oxygen sensing, have largely determined, and in some senses, limited sensor development. The bulk of the sensor technology falls under three classifications: fluorescence-dye optical, amperometric electrochemical, and thin film solid-state conductivity. Towards biochemical and biological applications, the first two types dominate, largely due to their inherent low oxygen concentration sensitivity and liquid-tolerance. Thin-film conductivity oxygen sensors such as tin dioxide film sensors have mainly seen application in environmental and combustion exhaust monitoring applications.<sup>1–7</sup>

Regarding biological applications such as water quality testing and fermentation monitors, the majority of commercially available oxygen sensors are still electrochemically-based. However, these sensors have severe limitations and suffer from problems such as fouling by organic matter, which leads to catastrophic failure and short operational lifetimes.<sup>8</sup>

Additionally, these types of sensors require a reference electrode, usually in the form of a silver–silver chloride electrode, which has been demonstrated to be difficult to miniaturize.<sup>9–10</sup> Other inherent problems exist with these sensors, such as analyte depletion during measurement, as electrochemical oxygen sensors rely upon the conversion of oxygen to hydroxyl ions, thus significantly reducing the actual oxygen concentration in small volumes.

Fluorescent oxygen-quenching sensors have been rapidly developed recently, due to their inherent high sensitivity, selectivity and stability. The majority of fluorescent dyes display oxygen-quenching characteristics, but discrete groups of molecules have shown enhanced sensitivity to oxygen, as well as relatively long fluorescent lifetimes, thus reducing the requirements of the optical transducers. These compounds are almost all organometallic in nature, although a few metal-porphyrin and pyridyl-based compounds display similar characteristics.<sup>11–18</sup> Studies on the effects of oxygen concentration on fluorescent lifetimes have also been carried out, but application of this technique remains limited by the complicated and expensive lifetime-sensing apparatus required.<sup>19</sup>

### 1.2 Integrated optical sensors

The need for effective, miniaturized and simple sensors has driven a massive research effort with systems varying in both principal of operation and morphology. However, despite recent advances in the field of MEMS-based sensors, the fabrication of miniaturized optical biosensors still tends to be a relatively difficult process, limited largely by complicated device fabrication and packaging.<sup>20–22</sup> Optical biosensors are particularly difficult to fabricate, as coupling light into microsystems typically requires accurate alignment components, such as micro-positioning stages for end-fire coupling.<sup>23–25</sup> Elements such as grating couplers and V-groove couplers may alleviate some of these difficulties, but are challenging and often impossible to integrate into existing microsystems.<sup>26–27</sup>

A simple method to embed an optical sensor in an existing biosensor system is an integrated optical waveguide, which can

allow light to be effectively conducted to a select point of interest within the device with minimal interference. Applications for this type of optical sensor include micro total-analysis systems ( $\mu$ TAS) and chemical sensing within separation channels, miniaturized bioreactors or artificial tissue culture substrates.<sup>28–32</sup> Quantitative analysis by integrated optical systems is also possible using fluorescent intensity sensing with a chemical specific dye immobilized at the tip or on the surface of the optical waveguide.<sup>33</sup>

Focusing on biochemical sensors, optical sensors have displayed advantageous characteristics, such as ultra low-concentration analyte sensitivity and flexibility, and with fluorescent sensors, high selectivity.<sup>16</sup> Due to their inherent high sensitivity, selectivity and stability, fluorescent sensors have rapidly been integrated into highly accurate, quantitative biochemical sensors.<sup>15</sup> However, to maximize the usage of a fluorescent sensor within a microscale device, three major obstacles must be overcome: immobilization of the dye at the point of interest in the microsystem, immobilization of a sufficient quantity of dye molecules, and conduction of light to the immobilized dye from illumination sources and back to light-sensitive components.

### 1.3 SU-8 Waveguides

The most efficient method to accomplish optical waveguide integration into a system is fabrication of the waveguides as part of the system. The advantage of this approach is lower coupling losses and less interference with the performance of the existing microsystem. In this work, an evanescent type interaction is used, which requires that a chemical-sensitive dye be immobilized on the surface of the waveguide. A diagram of this interaction is shown in Fig. 1.

As light is conducted down the integrated waveguide, the transverse energy field extends past the waveguide core boundaries into the surrounding substrate and dye layer. The evanescent energy field excites the dye molecules resulting in fluorescence emission and this emitted energy is superimposed on the transmitted light signal. The emitted signal from the waveguide contains components of the residual excitation signal and the fluorescent emission. Using simple filtering, chemical effects on the immobilized dye resulting in a change in fluorescent emission intensity and output spectra allow determination of specific interactions occurring at the waveguide surface. However, for the waveguide sensor to operate effectively, the waveguide must confine the light within the waveguide by total internal reflection while allowing transmission of a substantial portion—at least 80% for short waveguide structures—of the light at both excitation and emission frequencies. The material chosen for this study, the chemically-amplified, epoxy-based negative photoresist SU-8 possesses a relatively high refractive index of 1.80 as compared to the glass substrate of 1.46, and transmits over 94% of light above 400 nm. Additionally, SU-8 is patterned with established photolithography processes, using simple processing techniques, and thus is capable of successful integration into established microsystems. The fully polymerized resist is very stable in organic solvents,

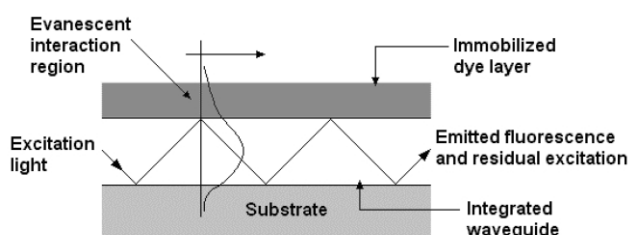


Fig. 1 Evanescent wave interaction.

allowing it to be used in adverse chemical and biochemical environments.

### 1.4 Layer-by-layer spin formation

For the integrated waveguide to operate as an evanescent fluorescent sensing system, the fluorophore must be immobilized along the waveguide surface. Interactions such as fluorophore excitation with materials immobilized on the surface of the waveguide can thus take place. To immobilize the dye, a combination of spin coating coupled with electrostatic interlayer attraction and interpolyelectrolyte formation was used. This technique is a variation of layer-by-layer formation by electrostatic self-assembly of alternately charged polyions.

Electrostatic layer-by-layer (ELBL) self-assembly technique is based upon the electrostatic attraction of ionically charged sites on a polymeric molecule to other charged species. These molecules, known collectively as *polyions*, exist in two forms, polycations, and polyanions, in reference to the positive or negative charges that exist along their chain structure. Adsorption of the first polyion layer takes place when the charged sites of the first polyion are electrostatically attracted to oppositely charged sites on the substrate surface. However, the number of charged sites on the polyion far outweighs the number on the substrate surface, and the remaining sites project away from the surface. This phenomenon of incomplete neutralization is essential to further adsorption and multilayer formation.<sup>34</sup> The remaining polyion charged sites induce a net surface charge, reversing the overall surface charge, and preventing any further polyion adsorption. Thus, a monolayer of polyions is formed on the substrate surface. A polyion of opposite charge to the first can then be applied to and be adsorbed to the surface, also being incompletely neutralized, and again reversing the surface charge. The process of incomplete neutralization and surface charge inversion can be performed indefinitely, thus permitting the formation of polyion multilayers.

Entrapment of dye molecules within the polyion multilayers can be achieved by pre-mixing the dye with an oppositely charged polyion to form stable inter-molecular bonds between them. The excess charges on the polyions allow continued surface adsorption and multilayer formation.<sup>15</sup> This technique, known as interpolyelectrolyte formation is shown in Fig. 2.

Interpolyelectrolyte complexes have net charges similar to the polyions used to form them, and are similar in form to a branched polymeric molecule. To ensure that the trapped molecule does not completely neutralize the polyion, a polyion that is long enough to retain excess charged sites after complex formation must be chosen. The entire complex thus has the ability to adsorb to an oppositely charged surface, leaving excess charged sites on its outer surface.

For surface adsorption to take place, the substrate must possess a surface charge opposite to that of the molecules to be adsorbed. The waveguide material used in this work, SU-8, does not possess the charged sites necessary to initiate self-assembly, and thus the electrostatic-self assembly process was augmented by spinning the polyions onto the surface of the substrate, and annealing them to the surface by heating. To provide an initial surface charge on the SU-8, the substrate was immersed in concentrated  $H_2SO_4$  for a short period, inducing the formation of charged surface groups, as described in the following section.

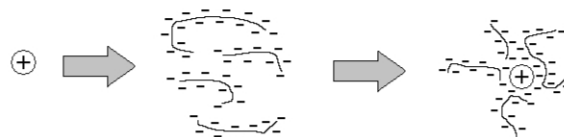


Fig. 2 Interpolyelectrolyte formation.

## Methodology

### 2.1 SU-8 surface modification

The waveguide core material SU-8 is an electrostatically neutral material at the required environmental pH of 7.6. To induce a surface charge, the fabricated waveguides were soaked for 3–5 s in 95% H<sub>2</sub>SO<sub>4</sub> at 85 °C. This treatment generated negatively charged phenol and glycol groups on the surface of the waveguide, facilitating polyion–surface adhesion, as shown in Fig. 3. However, since extended immersion in hot H<sub>2</sub>SO<sub>4</sub> dissolves SU-8, insufficient charged surface groups were formed for efficient self-assembly, and thus spin coating of the polyions was required to form the multilayer film on the waveguide surface.

### 2.2 Multilayer materials

The fluorophore used for this study was the oxygen-sensitive dye tris(2,2'-bipyridyl dichlororuthenium) hexahydrate (Ru(bpy)), purchased from Aldrich Chemical Company in crystalline form and used in solution mixed with the polyanion poly(sodium styrenesulfonate) (PSS) at concentration of 0.57 mg ml<sup>-1</sup>. The polycation used was the chemical poly(diallyl dimethylammonium) chloride (PDDA), and the initial polyion layer was composed of the polycation poly(ethylenimine) (PEI). The specifications for the polyions used were as follows: PEI of molecular weight 70 000 at 1.5 mg ml<sup>-1</sup>, PSS of molecular weight 500 000 at 3 mg ml<sup>-1</sup>, and PDDA of molecular weight 70 000 at 2 mg mL<sup>-1</sup> (Sigma-Aldrich Chemical). All the polyions used in this study were strongly charged at pH 6–8.<sup>35</sup> The chemical structures for the dye and polyions used are given in Fig. 4.

The initial five layers that were applied to the waveguides consisted of PEI, followed by a pair of PSS/PDDA bilayers. The

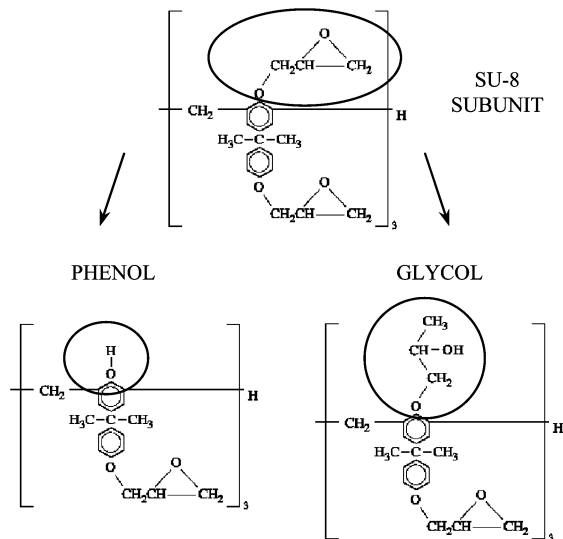


Fig. 3 Chemical modification of SU-8 at waveguide surface.

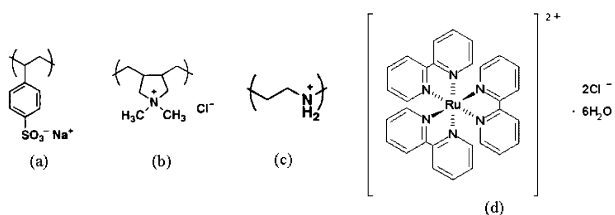


Fig. 4 Structural images of polyion and dye molecules: (a) poly(sodium styrenesulfonate), (b) poly(diallyl dimethylammonium)chloride, (c) poly(ethylenimine) and (d) tris(2,2'-bipyridyl dichlororuthenium) hexahydrate.

purpose of these preparatory layers was to overlap charge non-uniformities on the waveguide, thus providing a uniform surface charge for the successive dye-impregnated polyion multilayers. Twenty functional bilayers were applied to the surface of the waveguides, for a total of 45 monolayers.

### 2.3 Multilayer spin-coat formation

The spin-coating process was adopted from work by Chiarelli and coworkers, and is fundamentally different from self-assembly.<sup>36</sup> Self-assembly of the dye onto optical substrates was previously optimized for layer number and dye concentration by Chang-Yen and coworkers.<sup>15</sup> This type of monolayer formation assembly uses the electrostatic attraction between the alternately charged polyion layers to adsorb polyion material from solution onto the substrate solution to form a solid film. However, since the surface charge of the H<sub>2</sub>SO<sub>4</sub>-treated SU-8 was insufficient to cause adsorption, the polyion solutions were each spun onto the surface of the substrate at 200 rpm for 60 s, then heated for 1 min at 105 °C to anneal the film. Annealing improved interlayer adhesion by increasing the interpenetration between the films, augmenting the stability of the multilayer film. The electrostatic attraction between the polyion monolayers thus takes a secondary role in the film formation as the interlayer stabilizing force instead of the formation mechanism.

Following the complete multilayer formation process, the substrate was immersed in buffered water at pH 7.6 to observe if any dye desorption took place. After three hours, a small amount of dye was observed in the water, with no further desorption after six hours.

### 2.4 Waveguide fabrication and fiber-optic coupling

A unique approach to the fabrication of the waveguides and optical interfaces was used for this work. A method was developed combining two manufacturing steps, waveguide fabrication and fiber-optic interfacing, into a single process. The monolithic nature of the integrated optics helps to increase robustness. Additionally designed into this single process was the self-aligning ability of the interfacing fiber optics with the integrated waveguides, allowing the device optics to be assembled by hand with minimal difficulties.<sup>37</sup> Finally, the inherent simplicity of the merged process greatly decreased the project complexity, thus improving the device yield, while facilitating the rapid fabrication of large numbers of the optical elements. The SU-8 waveguides/couplers were produced using a single lithographic mask on a 1" × 1.5" microscope slide (Fisher Scientific), and coupled with 50 μm core-125 μm cladding multimode optical fiber (Thorlabs). The mask pattern produced 20 waveguides per chip and yield generally was 100%, although only a single waveguide was used at a time. A diagram of the waveguide/coupling system is shown in Fig. 5. The tapered optical fiber interfaces allowed rapid assembly of the system using no specialized alignment stages—the optical fibers were inserted into the tapered and self-guided to the integrated waveguide interface region. To fix the fibers in

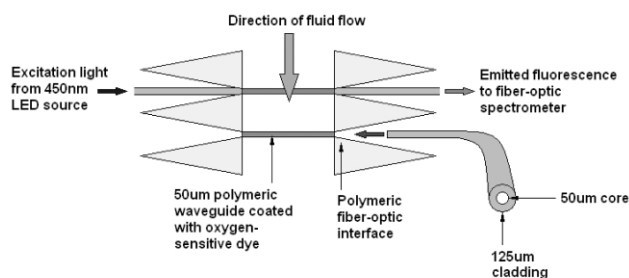


Fig. 5 Waveguide/coupling system.

position, a small amount of SU-8 was used as an adhesive. The use of SU-8 as the adhesive had the advantage of not introducing any additional optical interfaces and the accompanying losses between the fiber optics and the waveguides.

## 2.5 Fluid coupling

Continuing with the precept of simple and rapid device fabrication, the microfluidic channel was constructed from poly(dimethyl siloxane) (PDMS) using a single-stage casting process. Fluid inlet and outlet ports were integrated into the cast, further shortening the device construction time. The waveguide/flow cell was assembled into a controlled dissolved oxygen apparatus for sensitivity testing, as shown in Fig. 6.<sup>38–40</sup>

The dissolved oxygen concentration in water buffered at pH 7.6 was varied from 0.8 to 24.8 mg l<sup>-1</sup> by controlling the ratio of bubbled oxygen and nitrogen into the mixing chamber, which was monitored with a Traceable® dissolved oxygen probe (VWR Scientific). Once the dissolved oxygen concentration had stabilized to a set value, the dye was excited by the 450 nm LED source, and the emitted fluorescence was detected by the USB spectrometer (Oceanoptics), using a 5 s integration period with ten averaged samples and a 30 point boxcar average. The total 50 s sample period was longer than the response of the dye,

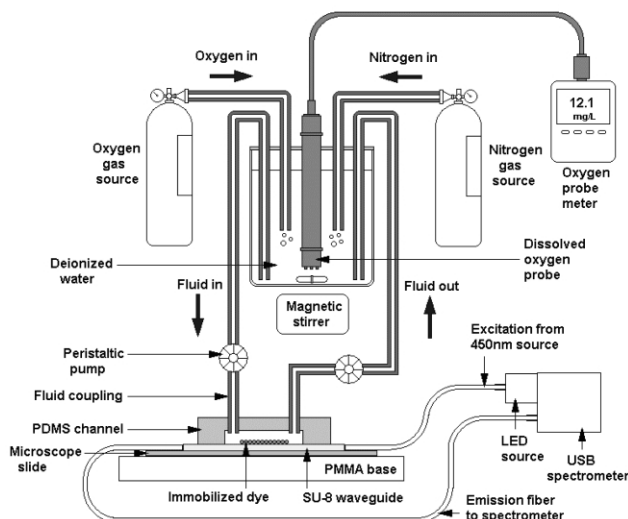


Fig. 6 Schematic of controlled dissolved oxygen apparatus.

and thus the system effectively responded immediately to changes in dissolved oxygen concentration. The fluorescence signal strength was extracted from the output spectra, normalized and correlated with the known dissolved oxygen concentrations to produce a calibration plot.

## Results

The assembled integrated waveguide, spectrometer and fluidic channel system is shown in Fig. 7. Water buffered at pH 7.6 is flowed through the PDMS channel via 1/16" tubing entering and exiting from the right of the photograph. The entire spectrometer and integrated waveguide/flow cell system was enclosed in a light-tight box to reduce the interference by external light sources.

The normalized fluorescence–oxygen concentration response calibration plot at the fluorescence wavelength of 615.27 nm is shown in Fig. 8. Normalization of the fluorescence intensity was achieved by dividing the intensity values into the maximum fluorescence value, to determine if a trend consistent with the Stern–Volmer relationship was present.<sup>40</sup>

$$\frac{I_0}{I} = 1 + K_{SV}[O_2] \quad (1)$$

The inset shows the excitation and intensity spectra. The large separation between the excitation and emission peaks—approximately 150 nm—allowed us to dispense with the excitation filter at the detector.

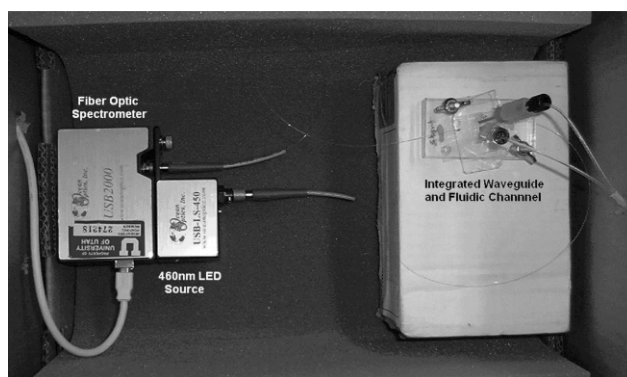


Fig. 7 Assembled oxygen sensor-controlled dissolved oxygen is pumped through the fluidic channel via tubes to the right.

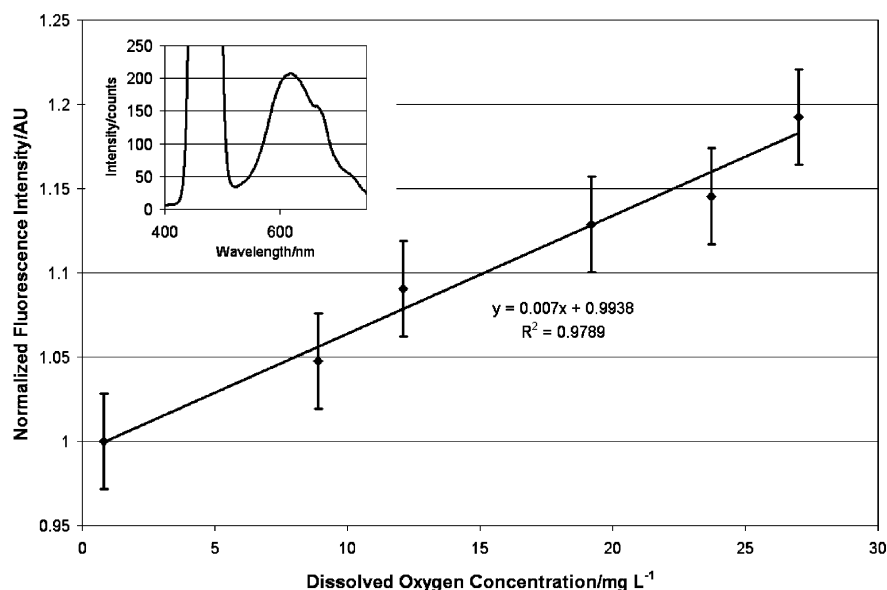


Fig. 8 Normalized fluorescence–oxygen concentration response calibration plot (Inset: fluorescence response).

Comparing the fluorescent response of the system with previous work using the same dye and a non-evanescent optical arrangement, the evanescent system is capable of detecting approximately seven times less fluorescent intensity than the non-evanescent system, but with a 10-fold reduction in standard error.<sup>15</sup> The calibration plot shows a strong linear correlation between the changing oxygen concentration and the normalized fluorescence emission intensity, following the Stern–Volmer relationship and indicating successful oxygen sensing by the system. The maximum resolution of the system can be calculated from the calibration data as a change of approximately 0.6 mg l<sup>-1</sup> (600 ppb) dissolved oxygen concentration. Although not shown, the changes in fluorescent intensity were relatively small compared with the total fluorescence. The maximum dissolved oxygen concentration that the apparatus was capable of producing (24.8 mg l<sup>-1</sup>, corresponding to approximately 19 mTorr) only caused a 16% decrease in total fluorescent output. While this range includes most applications of interest, such as cell culture, future investigations are planned to exploit the full output range, as well as optimization of the optical apparatus to expand this range. The sensor showed no measurable drift over the two day period of sampling, and random testing of similar data points at multiple times did not uncover any significant variation.

Towards system instrumentation improvements, either using a longer integration time or replacing the spectrometer with a low-pass filter and a photomultiplier tube can increase this resolution. However, these changes would increase the time response of the sensor and complexity of the system, respectively. The range of oxygen concentration used for this study was relatively large, which allows this sensing technique to be used for a wide variety of oxygen-sensing applications. Concentrations of dissolved oxygen to support aquatic life fall well within the range of this sensor,<sup>41</sup> and ruthenium-based oxygen sensing systems such as the Oxford Optronics Oxy-lite<sup>®</sup> are currently being used to probe oxygen concentrations in cell cultures as high as 100 Torr.<sup>42</sup> Additionally, due to the large optical transmission range of SU-8, any fluorophore that excites using a wavelength longer than 400 nm is capable of operating with this system.

## Conclusions

A polymeric integrated optical evanescent waveguide sensor for dissolved oxygen was fabricated using a single stage lithographic process. Dye immobilization on the waveguide surface was achieved using a combined spin assembly/layer-by-layer deposition with interpolyelectrolyte formation. The assembled waveguide sensor successfully demonstrated oxygen sensitivity over a range of 0.8 to 24.8 mg l<sup>-1</sup> with a strongly linear response. Possible applications for this type of optical sensor vary from micro total-analysis systems ( $\mu$ TAS), chemical-sensing within separation channels or miniaturized bioreactors and artificial tissue culture substrates. For commercial applications, the Oceanoptics spectrometer would be replaced by a simple filter and photodiode sensor, and the entire system would be fabricated in a sealed chamber with ports for fluid and electrical connections. The compactness of the sensor would lend to both ease of use and the ability to integrate it into portable analysis systems. The waveguide material SU-8 is however not desirable in manufacturing situations, as the developer is toxic and relatively time-consuming photolithographic methods are required. To make the fabrication of this sensor more viable commercially, we are investigating a molding process to construct the waveguides using PDMS, which is also transparent to UV and visible light, but does not require exposure or development processes. The fabrication and assembly techniques used in this work are inherently generic and have the potential for use in a wide range of

systems. We are therefore exploring the application of this technique to several biochemical and biowarfare agent detection problems and expect that the system will find application in a wide range of other applications.

## References

- 1 T. Becker, S. Muhlberger, C. Bosch-v. Braunmuhl, G. Muller, T. Ziemann and K. V. Hechtenberg, *Sens. Actuators, B*, 2000, **69**, 108.
- 2 R. Moos, W. Menesklou, H.-J. Schreiner and K. H. Hardtl, *Sens. Actuators, B*, 2000, **67**, 178.
- 3 G. Reinhardt, I. Rohlfis, R. Mayer and W. Gopel, *Sens. Actuators, B*, 2000, **65**, 76.
- 4 S. I. Somov, G. Reinhardt, U. Guth and W. Gopel, *Sens. Actuators, B*, 2000, **65**, 68.
- 5 A. L. Spetz, P. Tobias, L. Uneas, H. Svenningstorp, L.-G. Ekedahl and I. Lundstrom, *Sens. Actuators, B*, 2000, **70**, 67.
- 6 H. Zheng and O. T. Sorensen, *Sens. Actuators, B*, 2000, **65**, 299.
- 7 L. Zheng, M. Xu and T. Xu, *Sens. Actuators, B*, 2000, **66**, 28.
- 8 P. R. Warburton, R. S. Sawtell, A. Watson and A. Q. Wang, *Sens. Actuators, B*, 2001, **72**, 197.
- 9 T. Hermes, M. Buhner, S. Bucher, C. Sundermeier, C. Dumschat, M. Borchardt, K. Cammann and M. Knoll, *Sens. Actuators, B*, 1994, **21**, 33.
- 10 H. Suzuki, T. Hirakawa, T. Hoshi and H. Toyooka, *Sens. Actuators, B*, 2001, **76**, 565.
- 11 P. Douglas and K. Eaton, *Sens. Actuators, B*, 2002, **82**, 200.
- 12 P. Douglas and K. Eaton, *Sens. Actuators, B*, 2002, **82**, 48.
- 13 K. Eaton and P. Douglas, *Sens. Actuators, B*, 2001, **82**, 94.
- 14 Y. Amao, K. Asai, T. Miyashita and I. Okura, *Polym. Adv. Technol.*, 2000, **11**, 705.
- 15 D. Chang-Yen, Y. Lvov, M. McShane and B. Gale, *Sens. Actuators, B*, 2002, **87**, 336.
- 16 R. Carswell and A. R. Khoie, *Soc. Photo-Opt. Instrum.*, 1996, **2705**, 22.
- 17 Z. Murtaza and J. R. Lakowicz, *Soc. Photo-Opt. Instrum.*, 1999, **3602**, 326.
- 18 M. T. Murtaugh, H. C. Kwon and M. R. Shahriari, *Soc. Photo-Opt. Instrum.*, 1997, **3136**, 187.
- 19 P. Hartmann, W. Ziegler, G. Holst and D. W. Lubbers, *Sens. Actuators, B*, 1997, **38–39**, 110.
- 20 J. M. Eighenholz, *Adv. Packaging*, 2002, **11**, 27.
- 21 D. I. Amey, B. E. Taylor, D. M. Horowitz and J. Samuel, *Adv. Packaging*, 2002, **11**, 30.
- 22 M. Robert, *Proc. SPIE*, 1999, **3891**, 22.
- 23 B. Rose and O. Leistiko, *Proc. SPIE*, 1996, **2686**, 175.
- 24 Y. Zhou, Y. L. Lam, S. D. Cheng and C. H. Kam, *Proc. SPIE*, 1998, **3491**, 1163.
- 25 J. Mueller, D. Zurhelle, K. Fischer, A. Loeffler-Peters and R. Hoffmann, *Proc. SPIE*, 1993, **1794**, 167.
- 26 S. Goel and D. L. Naylor, *Proc. SPIE*, 1991, **1396**, 404.
- 27 J. Backlund, *Dokl. Chal. Tekn. Hkla.*, 2001, **1714**, 48.
- 28 O. Kohls and T. Scheper, *Sens. Actuators, B*, 2000, **70**, 121.
- 29 B. A. A. Dremel, S.-Y. Li and R. D. Schmid, *Biosens. Bioelectron.*, 1992, **7**, 133.
- 30 M. Li, H. Ai, D. K. Mills, Y. M. Lvov, M. J. McShane and B. K. Gale, *Proc. 2nd Ann. Intl. IEEE-EMBS Spec. Topic Conf. Microtech. Med. and Biol.*, Madison, Wisconsin, USA, 2002, 109.
- 31 F. Loth, S. A. Jones, D. P. Giddens, H. Bassiouny, S. Glagov and C. K. Zarins, *J. Biomech. Eng.*, 1997, **119**, 187.
- 32 J. L. Ricci, A. G. Gona and H. Alexander, *J. Biomed. Mater. Res.*, 1991, **25**, 651.
- 33 A. Weber and J. S. Schultz, *Biosens. Bioelectron.*, 1992, **7**, 193.
- 34 H. M $\ddot{o}$ hwald, *Protein Architecture–Interfacing Molecular Assemblies and Immobilization Biotechnology*, 125, ed. Yuri Lvov, Marcell Dekker Inc., New York, 2000.
- 35 Y. Lvov, K. Ariga, I. Ichinose and T. Kunitake, *J. Am. Chem. Soc.*, 1995, **117**, 6117.
- 36 P. A. Chiarelli, M. S. Johal, D. J. Holmes, J. L. Casson, J. M. Robinson and H.-L. Wang, *Am. Chem. Soc.*, 2002, **18**, 168.
- 37 S. Camou, J. P. Gouy, H. Fujita and T. Fujii, *Proc. Sens. 2002*, Orlando, 2002, 1.
- 38 G. M. Whitesides, E. Ostuni, S. Takayama, X. Jiang and D. E. Ingber, *Ann. Rev. Biomed. Eng.*, 2001, **3**, 335.
- 39 D. J. Beebe, G. A. Mensing and G. M. Walker, *Ann. Rev. Biomed. Eng.*, 2002, **4**, 261.
- 40 A. Folch, *Ann. Rev. Biomed. Eng.*, 2000, **2**, 227.
- 41 1986 Quality Criteria for Water, EPA 440/5-86-001, May 1986.
- 42 H. M. Swartz, *Biochem. Soc. Trans.*, 2001, **30**, 248.